Biochemistry

 Volume 18, Number 15 July 24, 1979

Proton Nuclear Magnetic Resonance of Minor Nucleosides in Yeast Phenylalanine Transfer Ribonucleic Acid. Conformational Changes as a Consequence of Aminoacylation, Removal of the Y Base, and Codon–Anticodon Interaction†

Pari Davanloo,‡ Mathias Sprinzl,* and Friedrich Cramer

ABSTRACT: The assignments of the resonances of the methyl and methylene groups belonging to the residues dihydrouridine-16 and -17 (C_5 and C_6), dimethylguanosine-26, *N*-2-methylguanosine-10, and 7-methylguanosine-46 of yeast $tRNA^{Phe}$ at low temperature are reported. Observing the high-field proton NMR spectral region at different temperatures, the effects of aminoacylation, removal of the Y base, and codon–anticodon interaction on the tertiary structure of yeast $tRNA^{Phe}$ were investigated. The following are the results of this study. (1) The two dihydrouridine residues of $tRNA^{Phe}$ have different environments in aqueous solution: dihydrouridine-16 is more shielded than dihydrouridine-17. (2) The ribothymidine residue from the fragment (47–76) of yeast $tRNA^{Phe}$ and from a tRNA with a partially disrupted structure exhibits multiple conformations arising from different stacking modes between the ribothymidine-54 and the guanosine-53 residue. (3) Upon aminoacylation the type of guanosine-53 interaction with ribothymidine-54 in the $tRNA^{Phe}$ changes. (4) Removal of the Y base from the anticodon loop of yeast $tRNA^{Phe}$ weakens the thermal stability of the tertiary interactions. (5) The interaction of two complementary anticodons in the absence of proteins and of ribosomes results in stabilization of the tertiary structure. Codon–anticodon interaction dependent rearrangement of the tertiary structure of yeast $tRNA^{Phe}$ was not observed. The spin–lattice relaxation times of the methyl and methylene groups of the minor nucleosides in yeast $tRNA^{Phe}$ demonstrate that the minor nucleosides undergo rotational reorientation (τ_c) in the nanosecond range. The observed differences in these τ_c values indicate a similarity of structure of $tRNA^{Phe}$ in solution and in crystalline form.

The three-dimensional structure of tRNA based on X-ray crystallography of yeast $tRNA^{Phe}$ (Jack et al., 1976; Quigley et al., 1975) indicates that the G-T-Ψ-C-R sequence in the T-Ψ-C loop takes part in either secondary or tertiary hydrogen bonding and/or undergoes stacking with bases from the D loop. Therefore, it is not available for interaction with other molecules (Pongs et al., 1973). However, the experiments of Richter et al. (1973, 1974) and of Sprinzl et al. (1976) indicate that the T-Ψ-C-G sequence of tRNA is involved in the interaction with the 50S ribosomal subunit during the elongation process. Such interaction would imply a disengagement of the T-Ψ-C loop from the D loop during the ribosomal binding process.

It has been shown by equilibrium dialysis experiments (Schwarz et al., 1974, 1976; Schwarz & Gassen, 1977; Möller et al., 1978) that the codon–anticodon interaction triggers the conformational change in tRNA, exposing the T-Ψ-C-G sequence for binding to the oligonucleotide C-G-A-A and that the 30S ribosomes and EF-Tu·GTP are not necessary for this process. Further evidence for the above mechanism comes from base-specific chemical modification (Wagner & Garret, 1978) and also from fluorescence measurements using $tRNA^{Phe}$ containing an ethidium probe in the D loop (Robertson et al., 1977). On the other hand, the studies of Chin & Kidson (1971) and Dvorak et al. (1976) have suggested that aminoacylation induces unmasking of the sequence T-Ψ-C-G. In order to obtain physical evidence for such a conformational opening in the tRNA molecule as a result of codon–anticodon interaction and of aminoacylation, we have utilized the high-field NMR spectral region, which contains resonances from the minor nucleosides to monitor the structural changes in tRNA.

We have investigated the effect of complex formation between *Escherichia coli* $tRNA^{Glu}$ and yeast $tRNA^{Phe}$ on the proton NMR resonances of their respective minor nucleosides in the high-field region of the spectrum. These two tRNAs have complementary anticodons which lead to formation of a tight complex via anticodon–anticodon interaction (Eisinger,

† From the Max-Planck-Institut für experimentelle Medizin, Abteilung Chemie, D-3400 Göttingen, West Germany. *Received February 8, 1979.* This work was supported by the Deutsche Forschungsgemeinschaft (Cr 8/45).

‡ Present address: Biochemistry and Molecular Biology Department, Harvard University, Cambridge, MA 02138.

0006-2960/79/0418-3189$01.00/0

1971; Grosjean et al., 1976). This interaction between two anticodons can be used as a model for the codon–anticodon interaction during ribosomal translation.

Materials and Methods

tRNA Samples and tRNA Fragments. Highly purified $tRNA^{Phe}$ and $tRNA_2^{Ser}$ were obtained from baker's yeast by a previously published procedure (Schneider et al., 1972). $tRNA^{Glu}$ from *E. coli* was prepared according to Nishimura's procedure (Nishimura, 1971). $tRNA^{Phe}$ lacking the Y base was prepared by the method of Thiebe & Zachau (1968) and was then purified by chromatography on benzoylated DEAE-cellulose. The amino acid acceptor activity of tRNA molecules was measured by the method of Sprinzl & Cramer (1973). The acceptor activities of yeast $tRNA^{Phe}$, yeast $tRNA^{Phe}(-Y)$, yeast $tRNA_2^{Ser}$, and *E. coli* $tRNA^{Glu}$ were 1666, 1410, 1100, and 1585 pmol/A_{260} unit of tRNA, respectively. *E. coli* $tRNA_1^{Arg}$ was prepared according to Kruse et al. (1978) and accepted 1600 pmol of arginine per A_{260} unit of tRNA. *Thermus thermophilus* $tRNA^{fMet}$ (Watanabe et al., 1978) had an acceptor activity of 1615 pmol of methionine per A_{260} unit of tRNA. ^{14}C-Labeled amino acid of a specific activity of 50 mCi/mmol was purchased from Schwarz/Mann, Orangeburg, NY.

The dodecanucleotide fragment A-Cm-U-Gm-A-A-Y-A-Ψ-m^5C-U-Gp from yeast $tRNA^{Phe}$ was prepared as described by Maelicke et al. (1973). The fragment (47–76) of yeast $tRNA^{Phe}$ was prepared as described by Wintermeyer & Zachau (1970). Analysis of the nucleoside composition of the tRNA samples, of the $tRNA^{Phe}$ fragment (47–76), and of the dodecanucleotide fragment was performed on a nucleoside analyzer described by Uziel et al. (1968). The purity of the $tRNA^{Phe}$ fragment (47–76) was further examined by gel electrophoresis in 7 M urea (Sprinzl et al., 1975). As a result of alkaline treatment, the 1-methyladenosine in the $tRNA^{Phe}$ (47–76) fragment was partially converted to 6-*N*-methyladenosine which can be identified in the nucleoside analysis of the fragment.

$tRNA^{Phe}$-C-C-A(3′NH_2), terminating with 3′-deoxy-3′-aminoadenosine, was prepared as described by Sprinzl et al. (1977). Preparative phenylalanylation of this tRNA with homogeneous yeast phenylalanyl-tRNA synthetase was performed according to Sprinzl & Cramer (1973) to an extent of 1480 pmol of phenylalanine per A_{260} unit of tRNA. Phe-$tRNA^{Phe}$-C-C-A(3′NH_2) was isolated from the reaction mixture by chromatography on Sephadex A-25 and desalted by gel filtration through Bio-Gel P-2 (Sprinzl et al., 1977). This procedure is identical with that applied for the isolation of unmodified yeast $tRNA^{Phe}$-C-C-A from bulk yeast tRNA (Schneider et al., 1972). Since the isolation and workup procedure of nonaminoacylated $tRNA^{Phe}$ and Phe-$tRNA^{Phe}$-C-C-A(3′NH_2) are identical, a direct comparison of both structures by NMR measurements is possible and artefacts due to purification of tRNA can be excluded. As shown by RPC 5 column chromatography (Roe et al., 1973) and polyacrylamide gel electrophoresis (Sprinzl et al., 1975), the Phe-$tRNA^{Phe}$-C-C-A (3′NH_2) contained less than 10% uncharged species and had an intact polynucleotide chain.

Preparation of NMR Samples. The NMR samples were prepared by extensive dialysis (at 4 °C), first against 10 mM EDTA, 100 mM KCl, and 10 mM potassium phosphate, pH 6.6, and then against 100 mM KCl, 10 mM $MgCl_2$, and 10 mM potassium phosphate, pH 6.6. The samples (0.3 mL) were then lyophilized, dissolved in 99.9% D_2O (Merck, Darmstadt, West Germany), again lyophilized, redissolved in 0.3 mL of 99.9% D_2O, and transferred to a Wilmed 5-mm NMR tube.

In order to eliminate paramagnetic impurities, we first dialyzed extensively the yeast $tRNA^{Phe}$ sample for T_1 measurement against 100 mM EDTA, 200 mM KCl, and 10 mM potassium phosphate, pH 6.6, followed by a repeat of the above mentioned procedure. In the case of *E. coli* $tRNA^{Glu}$ the sample was heated at 45 °C for 30 min in NMR buffer and was then quenched in ice, prior to NMR experiment, in order to convert any denatured tRNA to the native conformer (Eisinger & Gross, 1975). The yeast $tRNA^{Phe}$ sample lacking Mg^{2+} was prepared by multiple dialysis, first against 100 mM EDTA, 200 mM KCl, and 10 mM potassium phosphate, pH 6.6, and then extensively against 200 mM KCl and 10 mM potassium phosphate, pH 6.6. Atomic absorption measurement of this sample shows 1 mol of Mg^{2+} per mol of tRNA.

Proton NMR Spectroscopy. Proton NMR spectra were recorded by using the Fourier transform (90° pulse; 2.7-s acquisition time; 5-s pulse delay; Quadrature phase detection) procedure on a Bruker WH-270-MHz spectrometer located at the Max-Planck-Institute for Biophysical Chemistry, Göttingen. Temperatures were measured before and after each run by using the chemical shift difference between the methylene and the hydroxyl protons of ethylene glycol (van Geet, 1968). The field was locked to D_2O in the solvent. Chemical shifts are reported with respect to DSS (4,4-dimethyl-4-silapentane-1-sulfonate). All proton NMR measurements were performed in D_2O with 100 mM KCl, 10 mM $MgCl_2$, and 10 mM potassium phosphate buffer, pH 6.6, unless otherwise indicated. The negative signs of all chemical shifts are omitted except in the figures.

Results

Assignments of the Methyl and Methylene Resonances in the Intact Yeast $tRNA^{Phe}$ at Low Temperature. The 270-MHz Fourier transform high-field NMR spectrum of yeast $tRNA^{Phe}$ was measured at different temperatures (Figure 1). The dependence of the chemical shifts on the temperature and the assignments of the resonances are given in Figure 2. The assignment of the resonances above the melting temperatures (95 °C) is identical with that of Kan et al. (1977). Below the melting temperatures (e.g., 60 °C spectrum in Figure 1), the peak assignments are as follows.

(1) C_5 and C_6 Methylene Groups of the Nucleosides D-16 and D-17 and Methyl Groups of the Nucleosides m^2G-10 and m_2^2G-26. A comparison of C_5 and C_6 methylene resonances from the dihydrouridines at the positions 16, 17, and 20 in the D loop of several tRNAs (Table I) allows one to assign these resonances in yeast $tRNA^{Phe}$ (Figure 1). In the spectrum of *T. thermophilus* $tRNA^{fMet}$ (Davanloo et al., 1979) which contains only one D residue at position 20, two resonances, at 3.0 and 2.84 ppm, were observed at low temperature, which at the melting temperature move to 3.46 and 2.64 ppm, respectively. These two resonances were assigned to the C_6 (3.0 ppm) and C_5 (2.84 ppm) methylene groups of the D residue. A similar behavior was observed for the C_6 and C_5 methylene groups of the D-16 and D-20:1 residues of yeast $tRNA_2^{Ser}$, but in this tRNA the D-16(C_5) and D-16(C_6) resonances are overlapped by the D-20:1(C_5) and D-20:1(C_6) resonances, respectively. This might imply that the residues D-16, D-20, and D-20:1 have similar environments. In analogy to the above tRNAs, in yeast $tRNA^{Phe}$ the peaks at 2.74 and 3.0 ppm were assigned to D-16,17(C_5) and D-16(C_6), respectively. The peak at 2.77 ppm was assigned to the m^2G-10 resonance. This peak overlaps the left edge of the triplet peak (2.74 ppm) belonging to the D-16,17(C_5). Furthermore, we will demonstrate in the

Table I: Comparison of the C_6 and C_5 Methylene Chemical Shifts (ppm; DSS) from the Dihydrouracil Residues of Several tRNAs at the Different Positions of the D Loop in the Temperature Range of 50–90 °C[a]

tRNA	temp (°C)	chemical shifts (ppm) D-16 C_6	D-16 C_5	D-17 C_6	D-17 C_5	D-20 C_6	D-20 C_5
Phe (yeast)[b]	50	3.0	2.74	3.4	2.74		
	90	3.49	2.66	3.49	2.66		
Val_1 (*E. coli*)[c]	50			3.65	2.74		
	90			3.49	2.70		
fMet (*T. thermophilus*)[b]	50					3.0	2.84
	90					3.46	2.64
Arg_1 (*E. coli*)[b]	50			3.64	2.77		
	90			3.43	2.64		
Ser_2 (yeast)[b,d]	50	2.86	2.76			2.86	2.76
	90	3.49	2.64			3.49	2.64

[a] The numbering of nucleotides in each tRNA sequence is according to tRNA^{Phe} from yeast (Gauss et al., 1979). [b] Solution condition: 100 mM KCl, 10 mM Mg^{2+}, and 10 mM potassium phosphate, pH 6.6. [c] The chemical shift data are taken from the report by Kastrup & Schmidt (1978). Solution condition: 250 mM NaCl, 10 mM sodium phosphate, and 0.4 mol of Mg^{2+} per mol of tRNA. [d] The resonances from D-16, D-20, and D-20:1 are superimposed.

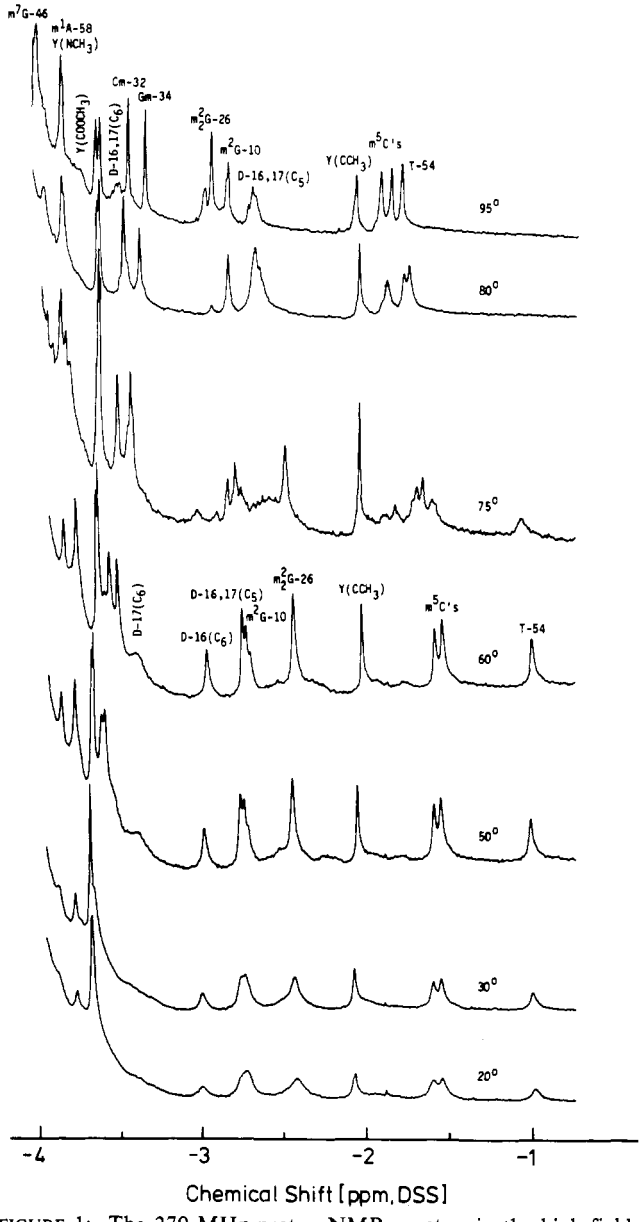

FIGURE 1: The 270-MHz proton NMR spectra, in the high-field region, of 0.55 mM yeast tRNA^{Phe} at various temperatures.

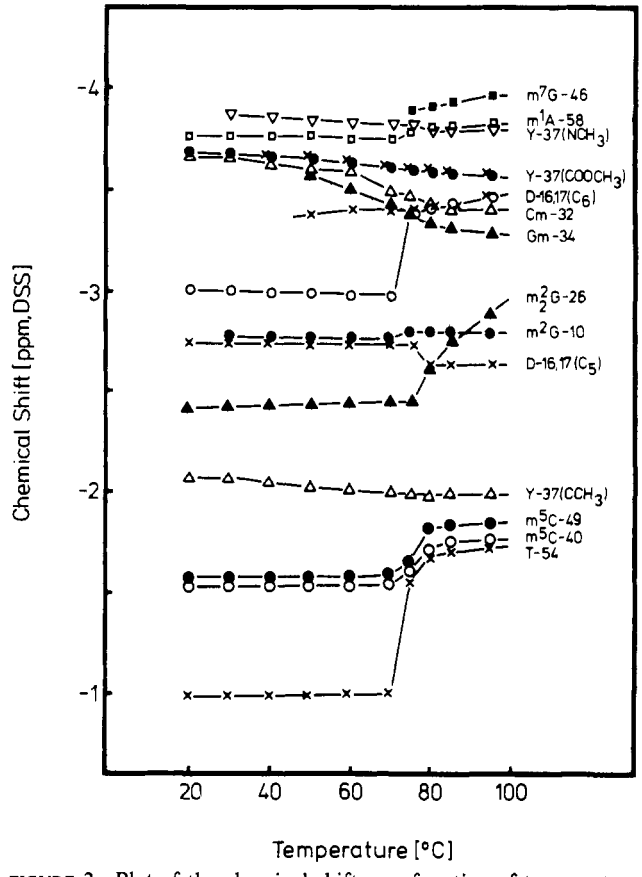

FIGURE 2: Plot of the chemical shift as a function of temperature for the resonances in Figure 1.

next section that the overlapping resonances resulting from residues D-16,17(C_5) and m^2G-10 can be separated in PRFT spectra as a result of appreciable differences in the T_1 values of these resonances. The peak at 2.43 ppm was then assigned to m_2^2G-26. This peak superimposes the resonance from the D-16,17(C_5) at 80 °C, and on a further rise in temperature to 95 °C it moved to 2.91 ppm with a downfield shift of 0.48 ppm upon unfolding.

Kan et al. (1977) have assigned the peak at 3.0 ppm to the C_6 methylene protons of D-16,17. We have observed that at 40 °C, beside the peak at 3.0 ppm, a broad peak at 3.4 ppm appears and its intensity increases until 70 °C. At 75 °C, the peaks at 3.4 and 3.0 ppm moved downfield and superimposed the Gm-34 resonance. At 95 °C, these resonances appear as a resolved triplet at 3.49 ppm. This observation leads us to speculate that in native intact tRNA^{Phe} the C_6 methylene

protons of D-16 and D-17 have different environments, one methylene being highly shielded ($\Delta\delta$ from 40 to 95 °C = 0.49 ppm) and the other being less shielded ($\Delta\delta$ from 40 to 95 °C = 0.09 ppm). The peak at 3.4 ppm (at 40 °C) is tentatively assigned to the C_6 methylene of nucleoside D-17. In support of this assignment, we have investigated the high-field proton NMR spectrum of *E. coli* $tRNA_1^{Arg}$ which contains a D-17 residue. In the region of 3–4 ppm, we have observed only one resolved triplet peak at 3.64 ppm, which was assigned to the C_6 methylene group of D-17. However, while the D-17(C_6) methylene group in $tRNA^{Arg}$ experiences an upfield shift of 0.21 ppm upon unfolding, the D-17(C_6) resonance in yeast $tRNA^{Phe}$ undergoes a slight downfield shift (0.09 ppm).

(*2*) *Methyl Groups of the Nucleosides Cm-32 and Gm-34.* At 20 °C Cm-32 and Gm-34 resonances superimpose the Y-37 ($2COOCH_3$). As the temperature is increased they shift upfield and at 60 °C are well separated. In a temperature range from 20 to 95 °C, we observed that in the presence of Mg^{2+} the Cm-32 and Gm-34 resonances shifted upfield by 0.25 and 0.36 ppm, respectively. This effect was not observed in the absence of Mg^{2+} (Robillard et al., 1977), indicating that in the presence of Mg^{2+} the nucleosides Cm and Gm in the anticodon loop are strongly stacked and that the Mg^{2+} plays an important role in the stabilization of the anticodon conformation. In the crystal structure of yeast $tRNA^{Phe}$, a strong Mg^{2+} binding site was identified in the anticodon loop (Quigley et al., 1978).

(*3*) *Methyl Groups of the Nucleosides m^7G-46 and m^1A-58.* In *E. coli* $tRNA^{fMet}$, lacking m^1A-58, we observed a peak at 3.79 ppm at low temperature which moved to 3.98 ppm at the melting temperature (Davanloo et al., 1979). This peak was assigned to the m^7G-46. It is therefore conceivable that in yeast $tRNA^{Phe}$ the m^7G-46 resonance superimposes the resonance of m^1A-58 (3.77 ppm) in a temperature range of 20–70 °C. At the melting temperature, the m^7G-46 is shifted to 3.99 ppm, which represents a downfield shift of 0.22 ppm upon unfolding.

(*4*) *Methyl Groups of the Nucleosides m^5C-40 and m^5C-49.* The assignment of m^5C-40 and m^5C-49 at the low temperature is still not resolved. All other assignments are in accordance with the previously reported work (Kan et al., 1977; Robillard et al., 1977).

^{1}H Spin–Lattice Relaxation Time Measurement of the Methyl and Methylene Groups in Yeast $tRNA^{Phe}$. ^{1}H spin–lattice relaxation times (T_1) of methyl and methylene groups in yeast $tRNA^{Phe}$ were determined from partially relaxed Fourier transform (PRFT) spectra (Vold et al., 1968; Allerhand et al., 1971), obtained by means of the 180° – t – 90° pulse sequence (Abragam, 1967). T_1 values were evaluated from the measurements of the peak heights from sets of PRFT spectra at different t by using the well-known expression (Abragam, 1967) shown in eq 1, where I_t and I_0 are

$$\ln (I_0 - I_t) = \ln 2I_0 - \frac{t}{T_1} \qquad (1)$$

the peak heights at time t and at equilibrium, respectively. The plots of log ($I_0 - I_t$) vs. t for the methyl and methylene groups of yeast $tRNA^{Phe}$ are shown in Figure 3. A straight line is obtained, which implies a single relaxation time for the methyl and methylene groups. The T_1 values which were evaluated by using least-squares analysis of all the data are given in Table II.

For the methyl and methylene protons of minor nucleosides in tRNA, the main cause of relaxation should be intramolecular dipolar interaction with protons within the same nucleoside unit. By making the assumption that a proton on a methyl group is relaxed only by those protons on the same carbon, then we can describe the relaxation time by eq 2

$$\frac{1}{NT_{1R}} = \frac{3}{10}\frac{\gamma_H^4\hbar^2}{r^6}\tau_c\left(\frac{1}{1+\omega_0^2\tau_c^2} + \frac{4}{1+4\omega_0^2\tau_c^2}\right) \qquad (2)$$

(Gutowsky & Woessner, 1956), where γ_H is the proton magnetogyric ratio (2.67×10^4 rad s^{-1} G^{-1}), r is the internuclear distance for the protons of a methyl group (1.78 Å), ω_0 is the NMR resonance frequency ($2\pi \times 270 \times 10^6$ rad/s), and N is the number of nuclei relaxing each proton ($N = 2$ for a CH_3 group). In the case of a methyl group, one has to consider two types of motion: first, the spinning of the methyl group about the bond linking it to the adjacent atom in the molecule (correlation time τ_{Me}) and, secondly, the rotational reorientation of the spinning axis (correlation time τ_c). Then, T_1 is given by eq 3

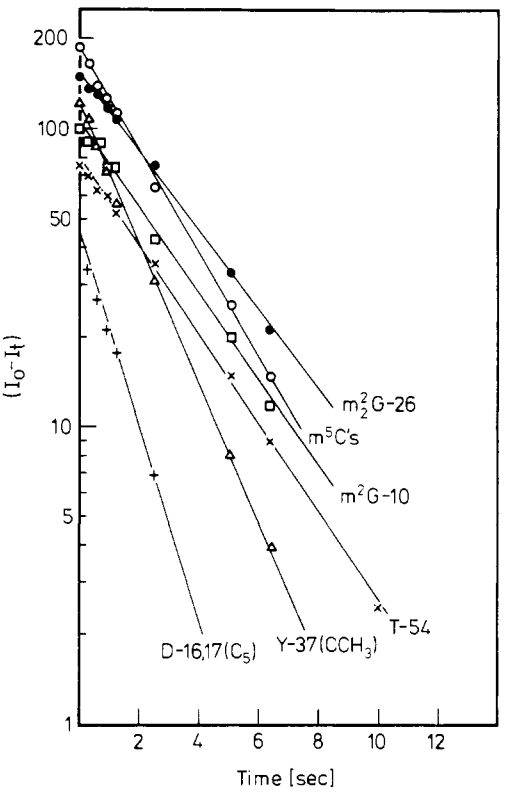

FIGURE 3: Semilogarithmic plots of ($I_0 - I_t$) vs. t (see eq 1) for the methyl and methylene groups of 0.55 mM yeast $tRNA^{Phe}$ in D_2O containing 200 mM KCl and 10 mM Mg^{2+} in 10 mM potassium phosphate buffer, pH 6.6, at T = 30 °C.

Table II: ^{1}H Spin–Lattice Relaxation Time Measurement of the Methyl and Methylene Groups of 0.55 mM Yeast $tRNA^{Phe}$ in D_2O with 10 mM Mg^{2+}, 200 mM KCl, and 10 mM Potassium Phosphate, pH 6.6, at 30 °C

minor nucleoside	T_1[a] (s)	τ_c (ns)
m_2^2G-26	3.23	7.5
T-54	2.95	7.0
m^5C's	2.57	6.2
Y-37(C_{11}-CH_3)	1.84	4.7
D-16,17(C_5-methylene)	1.31	5.7
m^2G-10	2.97	7.0

[a] The T_1 values of the methyl groups of the minor nucleosides which have a chemical shift between 3 and 3.9 ppm are not evaluated because of uncertainty in the base line, since these resonances are close to the steep slope of the ribose proton envelope.

$$\frac{1}{NT_1} = \frac{3}{10}\frac{\gamma_H^4\hbar^2}{r^6}\left[\left(\frac{1}{4}\right)\left(\frac{\tau_c}{1+\omega_0^2\tau_c^2}+\frac{3\tau_{c_1}}{1+\omega_0^2\tau_{c_1}^2}\right)+\left(\frac{\tau_c}{1+4\omega_0^2\tau_c^2}+\frac{3\tau_{c_1}}{1+4\omega_0^2\tau_{c_1}^2}\right)\right] \quad (3)$$

(Woessner, 1962) where

$$\frac{1}{\tau_{c_1}} = \frac{1}{\tau_c} + \frac{4}{\tau_{Me}}$$

In the case of the methyl group attached to a ring chromophore (Burke & Chan, 1970), the equation $\tau_{Me} \ll \tau_c$ is valid (for rapid spinning of the methyl group), and eq 3 is reduced to

$$\frac{1}{NT_1} = \frac{1}{4}\frac{1}{NT_{1R}}$$

In Figure 4, we show the log–log plot of NT_1 vs. τ_c. The dashed curve gives NT_1 which is calculated from eq 2 in the absence of spinning motion. The solid curve gives NT_1 which is calculated from eq 3 for the case when the methyl group is spinning very fast ($\tau_{Me} \ll \tau_c$).

In general, two real solutions (referred as "slow" and "fast" solutions) for τ_c can be calculated for each value of T_1 from eq 3. We have chosen the slow solution for τ_c based on the observed NMR line width of the methyl group resonance (full width at the half-height for T-54 at 30 °C is about 12 Hz). We have computed the τ_c, the correlation time for rotational reorientation of the spinning axis, from our measured T_1 value using the solid curve in Figure 4. The results are given in Table II (in the case of the C_5 methylene protons of D-16,17, τ_c is computed by using the dashed curve in the absence of spinning motion).

Studies of the Methyl Resonances from the Fragment (47–76) of Yeast tRNA^{Phe}. The temperature dependence of the high-field NMR of the fragment (47–76) of yeast tRNA^{Phe} in 10 mM Mg^{2+}, 100 mM KCl, and 10 mM potassium phosphate is presented in Figure 5. The methyl resonance of ribothymidine in the fragment passes through several different magnetic environments as the temperature is increased from 20 to 80 °C. At 20 °C two broad peaks (at 1.05 and 1.28 ppm) arising from this methyl group can be seen (Figure 5). On raising the temperature to 35 °C, we found that the peak at 1.05 ppm decreases in area, while the peak at 1.28 ppm becomes sharper and its area increases. At 45 °C a new peak at 1.32 ppm appears, and the peaks at 1.05 and 1.28 ppm decrease in area significantly. On raising the temperature further to 55 °C, the peaks at 1.05 and 1.28 ppm broaden, while the peak at 1.32 ppm reaches its maximum amplitude. Above 65 °C one peak can be seen which shifts downfield as the temperature is increased further.

As a result of the partial conversion of m^1A into m^6A during the preparation of the Phe fragment (47–76) (RajBhandary et al., 1968), two resonances at 3.87 and 2.96 ppm were observed which on the basis of the spectra of the corresponding nucleosides were assigned to the minor nucleosides m^1A and m^6A, respectively. No temperature dependence of these resonances was observed. The peak at 1.76 ppm, belonging to the nucleoside m^5C, exhibits a downfield shift of 0.23 ppm through the temperature range of 10–80 °C.

Comparison of the High-Field Spectral Region of tRNA^{Phe}-C-C, tRNA^{Phe}-C-C-A(3′NH$_2$), and Phe-tRNA^{Phe}-C-C-A(3′NH$_2$) with That of tRNA^{Phe}-C-C-A. In order to investigate the effect of aminoacylation on the high-field resonances of tRNA^{Phe}, we measured the proton NMR spectrum of Phe-tRNA^{Phe}-C-C-A(3′NH$_2$). The selection of this modified tRNA was determined by the fact that the amino acid residue is bound to the 3′-terminal A-76 through an amide bond, which cannot hydrolyze under the conditions of the measurement. The lability of the ester bond by which the phenylalanine is attached to native Phe-tRNA^{Phe}-C-C-A does not allow experiments in the wide temperature range which would be necessary for our comparative investigations. To exclude the possibility that the modification of the terminal adenosine residue and not its aminoacylation is responsible for any changes in the high-field NMR spectrum, we also screened the precursors of Phe-tRNA^{Phe}-C-C-A(3′NH$_2$), i.e.,

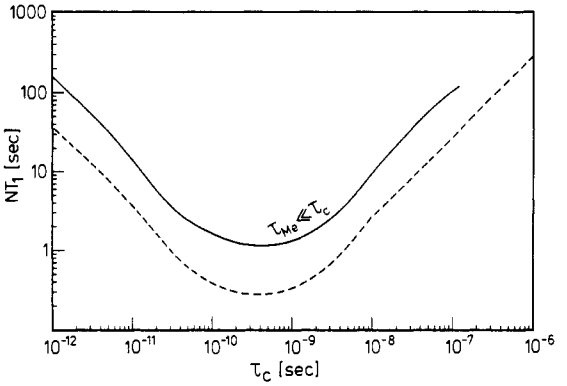

FIGURE 4: Log–log plot of NT_1 against τ_c for ω_0 = 270 MHz. The dashed curve (---) gives NT_1 values in the absence of the spinning motion (T_1 values are calculated from eq 2). The solid curve is for the case of fast methyl rotation ($\tau_{Me} \ll \tau_c$).

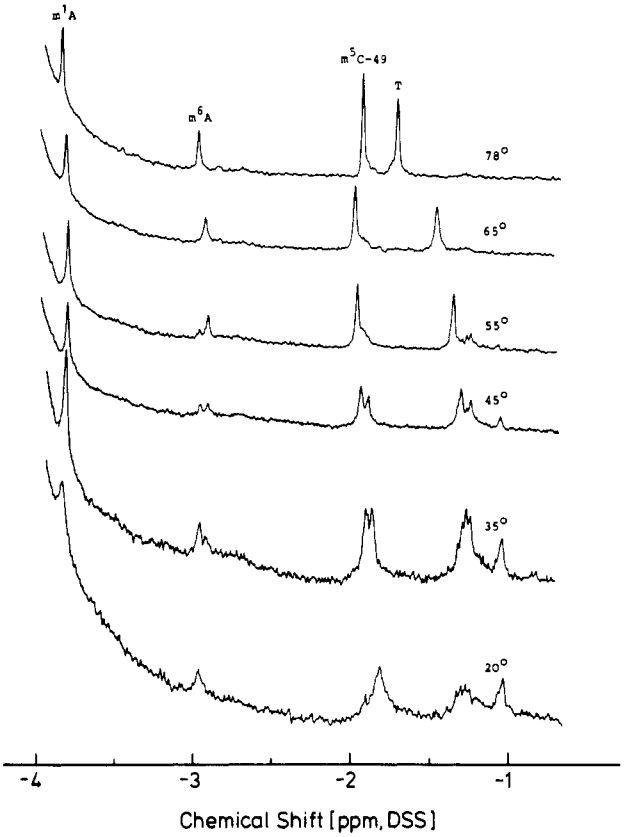

FIGURE 5: The 270-MHz proton NMR spectra of the methyl proton resonances from the minor nucleosides of the yeast tRNA^{Phe} (47–76) fragment at various temperatures (fragment concentration was 30 A_{260} units/0.3 mL).

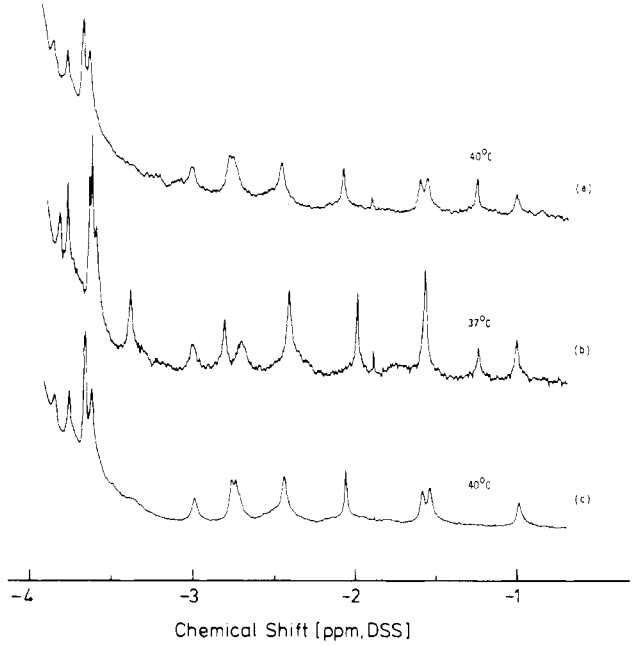

FIGURE 6: Comparison between proton NMR spectra, in the high-field region, of (a) Phe-tRNA^{Phe}-C-C-A(3′NH$_2$) in 100 mM KCl, 10 mM Mg^{2+}, and 10 mM potassium phosphate at pH 6.6 in D_2O; (b) yeast tRNA^{Phe} in 200 mM KCl, no Mg^{2+}, and 10 mM potassium phosphate at pH 6.6 in D_2O; and (c) yeast tRNA^{Phe} in the same buffer as described for (a).

tRNA^{Phe}-C-C and tRNA^{Phe}-C-C-A(3′NH$_2$). The high-field NMR spectra of these species are identical with that of the native tRNA^{Phe}-C-C-A in the temperature range from 30 to 90 °C (data are not shown).

Phe-tRNA^{Phe}-C-C-A(3′NH$_2$) shows a distinct difference in the region where the ribothymidine resonance should appear compared to the above nonaminoacylated species. All nonaminoacylated tRNAs exhibit a two-state transition upon melting in the presence of Mg^{2+}. This is reflected in ribothymidine resonance peaks at 1.0 (low temperature) and 1.72 ppm (high temperature). The Phe-tRNA^{Phe}-C-C-A(3′NH$_2$) spectrum, on the other hand, contains an additional resonance at 1.3 ppm at intermediate temperatures (Figure 6a). This resonance is assigned to the ribothymidine residue of Phe-tRNA^{Phe}-C-C-A(3′NH$_2$) on the basis of following observations. (a) The spectrum of the (47–76) fragment of tRNA^{Phe} (Figure 5) consists of peaks at 1.28 and 1.32 ppm in this region of the spectrum which could be assigned to the 5-methyl group of ribothymidine. (b) tRNA^{Phe}-C-C-A studied in the absence of Mg^{2+} (Figure 6b) exhibits a ribothymidine resonance at 1.3 ppm in its high-field spectrum. This resonance appears only at intermediate temperatures. *E. coli* tRNA^{Val}, measured in the absence of Mg^{2+} (Kastrup & Schmidt, 1978), also shows resonances in this region which were assigned to ribothymidine. (c) The resonance of ribothymidine at 1.3 ppm is present in the spectrum only at a certain temperature and is a component of transitions reflected in 1.0-, 1.3-, and 1.72-ppm resonances of the same residue. By raising the temperature, we found that the intensity of the 1.0-ppm resonance decreases concomitantly with the appearance of the 1.3-ppm resonance. At temperatures above the melting temperature, the 1.3-ppm resonance disappears and only the 1.72-ppm signal of ribothymidine remains in the spectrum.

We conclude from the above observations that the resonance at 1.3 ppm is due to ribothymidine which is in a conformation or in an environment different from that in which it occurs in the native tRNA^{Phe}-C-C-A in the presence of Mg^{2+} ions.

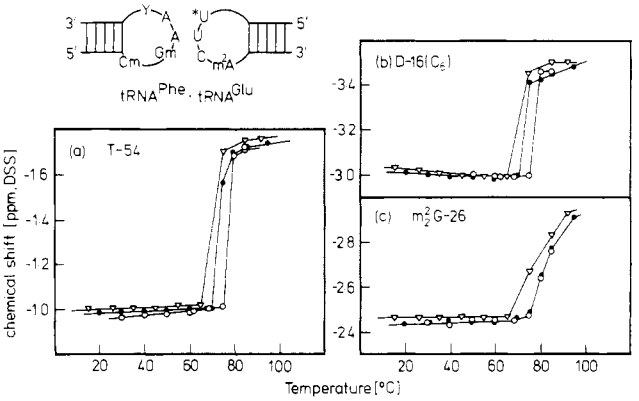

FIGURE 7: Effect of the removal of Y base and effect of the yeast tRNA^{Phe}·*E. coli* tRNA^{Glu} complex formation on the melting temperature of (a) T-54; (b) D-16(C_6); and (c) m_2^2G-26. (●) Yeast tRNA^{Phe} (0.55 mM); (▽) yeast tRNA^{Phe}(–Y) (0.55 mM); (○) yeast tRNA^{Phe}·*E. coli* tRNA^{Glu} complex (each 0.57 mM). Structures of the yeast tRNA^{Phe}·*E. coli* tRNA^{Glu} complex (anticodon regions) are shown above [U* is mam^{5}s^{2}U-34(NCH$_3$)].

The conformation of ribothymidine ascribed to the native tRNA^{Phe} and reflected in the 1.0-ppm resonance is not exclusively determined by the native tertiary structure of tRNA^{Phe}. This can be concluded from the observation that the (47–76) tRNA^{Phe} fragment also has a resonance typical for the native tRNA^{Phe} (Figures 1 and 6c) at 1.0 ppm (Figure 5). However, the resonance at 1.3 ppm is characteristic only of molecules where the tertiary structure is disrupted such as the (47–76) fragment of tRNA^{Phe} (Figure 5) or the intact tRNA^{Phe} species under conditions where the tertiary structure may be melted out (Riesner et al., 1973) (Figure 6b). On the basis of our control experiments and the analysis of Phe-tRNA^{Phe}-C-C-A(3′NH$_2$), we can exclude damage to the integrity of the polynucleotide chain of this tRNA during its preparation. Therefore, we conclude that the appearance of the 1.3-ppm ribothymidine resonance in the spectrum of this tRNA (Figure 6a) is due to its aminoacylation. The nonaminoacylated species does not show this resonance under identical conditions.

Effect of the Removal of the Y Base on the Proton NMR Spectrum of Minor Nucleosides in Yeast tRNA^{Phe}. The high-field NMR spectrum of yeast tRNA^{Phe}(–Y) was measured at different temperatures. The major changes compared to native tRNA^{Phe} are as follows. (a) Among the minor nucleosides in the anticodon loop, the temperature dependence of the Gm-34 peak is most affected when the Y base is removed. The Gm-34 resonance in the tRNA^{Phe}(–Y) at 50 °C has been shifted to a higher field by 0.2 ppm compared to native tRNA^{Phe}. The excision of Y base has, on the other hand, very little effect on the temperature dependence of the chemical shift of the Cm-32 resonance. This observation may indicate that the Gm-34 in the native tRNA^{Phe} participates in the stack involving the Y-37 and comprising the anticodon and its 3′ neighbors. Hence, as a result of the excision of the Y base, this stacking interaction is disrupted. (b) m^{5}C-49 and m^{5}C-40 resonances are superimposed at low temperatures (below 40 °C) and are less shielded in tRNA^{Phe}(–Y) than in native tRNA^{Phe}. (c) The resonances of T-54, m_2^2G-26, and D-16(C_6) in tRNA^{Phe}(–Y) show temperature-induced transitions lower by 3, 5, and 3 °C, respectively, than in the native tRNA^{Phe} (Figure 7). In general, the thermal denaturation of tRNA^{Phe}(–Y) takes place at a lower temperature than that of tRNA^{Phe}.

Effect on the Proton NMR Spectra of the Complex Formation between tRNAs with Complementary Anticodons. (1)

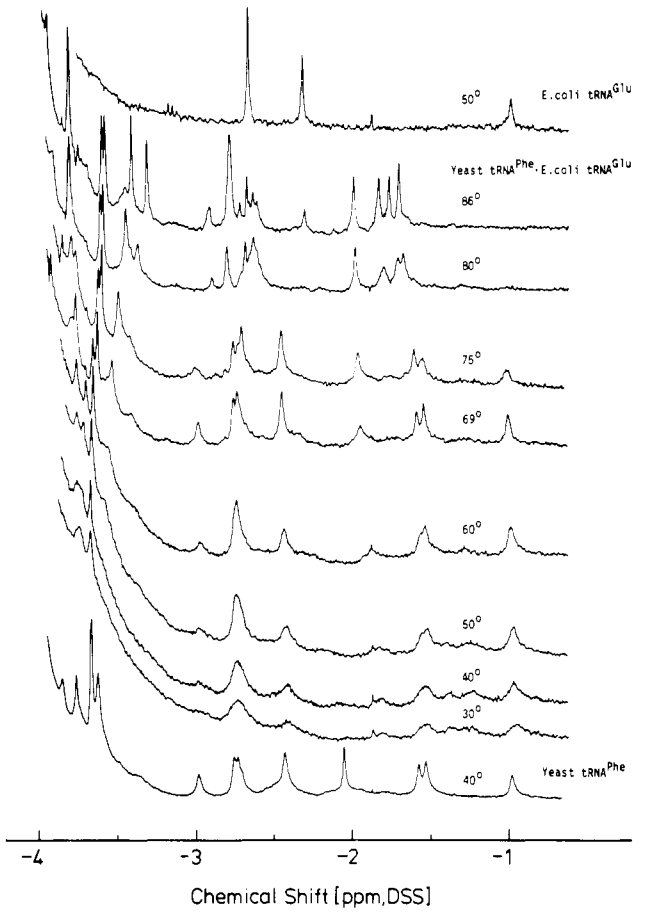

FIGURE 8: Temperature dependence of high-field 270-MHz proton NMR spectra of the yeast tRNA^{Phe}·*E. coli* tRNA^{Glu} complex, each 0.57 mM.

Assignments of the Resonances of E. coli tRNA^{Glu}. tRNA^{Glu} from *E. coli* contains 5-methyluridine (T-54), 2-methyladenosine (m^2A), and 5-(*N*-methylaminomethyl)-2-thiouridine (mam^5s^2U-34) in its sequence (Gauss et al., 1979). The relatively simple spectrum of *E. coli* tRNA^{Glu} at 50 °C (Figure 8) therefore contains only three major peaks in the region between 0 and 4 ppm from DSS. In analogy with the assignment of tRNA^{Phe} (Figure 1) and tRNA^{Val} (Kastrup & Schmidt, 1978), the peak at 1.0 ppm arises from the methyl protons of T-54. The peaks at 2.33, 4.0, and 2.68 ppm, which are not sensitive to temperature variations between 20 and 95 °C, were assigned to m^2A-37 and to the CH_2 and N-CH_3 resonances of mam^5s^2U-34, respectively. These assignments are based on the spectra of the free nucleosides in D_2O.

(2) E. coli tRNA^{Glu}·Yeast tRNA^{Phe} Complex. At equimolar concentrations, a complex of these two tRNAs species is formed due to complementarity of their anticodons (Grosjean et al., 1976). At the concentration of 0.57 mM of each tRNA in the NMR experiment, the expected melting of the tRNA^{Phe}·tRNA^{Glu} complex should be around 77 °C by using the temperature-jump data provided by Grosjean et al. (1976).

The 270-MHz spectrum of the complex at various temperatures is shown in Figure 8. Compared to the spectrum of the individual tRNAs, the methyl and methylene resonances of all minor nucleosides show a strong broadening upon complex formation between *E. coli* tRNA^{Glu} and yeast tRNA^{Phe}. As expected, the resonances originating from the anticodon nucleosides or their neighbors are influenced most strongly.

A very broad peak at 1.83 ppm in the 30 °C spectrum (Figure 8) which gradually shifts downfield with increasing

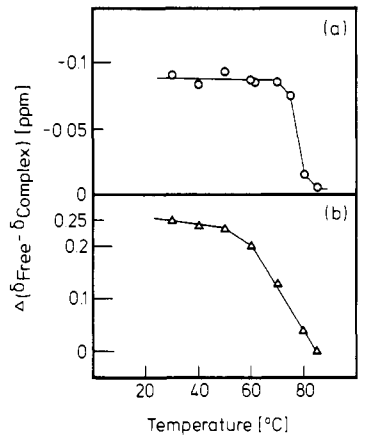

FIGURE 9: Plot of $\Delta(\delta_{free} - \delta_{complex})$ vs. temperature for (a) mam^5s^2U-34(NCH_3) proton resonance and (b) Y-37(C_{11}-CH_3) proton resonance in the tRNA^{Phe}·tRNA^{Glu} complex.

temperature belongs to the C_{11}-CH_3 resonance of Y-37 of tRNA^{Phe}. At 85 °C this resonance appears as a sharp peak at 2.0 ppm, corresponding to the chemical shift of the Y-37(C_{11}-CH_3) resonance in free tRNA^{Phe}. Hence, the upfield shift of about 0.25 ppm for Y-37(C_{11}-CH_3) can be used to monitor the tRNA^{Glu}·tRNA^{Phe} complex formation. The temperature-dependent changes in the position of this methyl group resonance in the complex as compared to that in the free tRNA^{Phe} are shown in the Figure 9b.

The *N*-methyl resonance of mam^5s^2U-34 of tRNA^{Glu} moves downfield by 0.09 ppm upon complex formation and superimposes the C_5 methylene proton resonances of D-16,17 of yeast tRNA^{Phe}. The plot of $\Delta(\delta_{free} - \delta_{complex})$ vs. temperature for the mam^5s^2U-34 proton resonance is shown in Figure 9a. While the mam^5s^2U-34 in the complex exhibits a narrow cooperative transition with the T_m around 78 °C, the Y-37(C_{11}-CH_3) shows a broad transition with the T_m around 73 °C (Figure 9a,b).

The resonance of the m^2A-37(C_2-CH_3) which is visible as a sharp peak in the 50 °C spectrum of free tRNA^{Glu} completely disappears from the spectrum of the tRNA^{Phe}·tRNA^{Glu} complex. This could be due either to superimposition of some other resonance or to strong broadening which makes the identification impossible. This resonance reappears in the 86 °C spectrum of the tRNA^{Phe}·tRNA^{Glu} complex. This behavior indicates the involvement of the m^2A residue in the interaction between the tRNAs and in addition a sharp monomer complex transition.

Due to the high density of the peaks in the region between 4 and 3.5 ppm and to a strong broadening at low temperature, it is difficult to perform an unambiguous assignment of resonances originating from other minor nucleosides in the anticodon loop of tRNA. However, the peak at 3.74 ppm in the 50 °C spectrum of the complex (Figure 8), which moves by 0.16 ppm upfield as the temperature increases, probably belongs to one of the ($COOCH_3$) methyl groups of Y-37. This assignment is based on the observation that in the 69 °C spectrum of the complex this peak is at 3.66 ppm, a position where the Y-37($COOCH_3$) resonance appears in the spectrum of free tRNA^{Phe} from yeast.

Broadening of the peaks upon complex formation was also observed for the methyl and methylene resonances of the minor nucleosides from parts of the tRNA other than the anticodon. For these minor nucleosides, however, no significant change in the chemical shift upon complex formation was detected. The resonance of the T-54 methyl group is shifted by only 0.015 ppm upfield, but the peak is much broader in the

complex at 50 °C as compared to the corresponding spectrum of free $tRNA^{Glu}$ or $tRNA^{Phe}$ (Figure 8).

The temperature vs. chemical shift dependence of some resonances is given in Figure 7. The melting of T-Ψ-C regions of the $tRNA^{Phe}$·$tRNA^{Glu}$ complex is reflected in a very sharp cooperative transition at 78 °C. The melting, as monitored by the change of the chemical shift of T-54 of yeast $tRNA^{Phe}$, takes place at a temperature 5 °C higher in the complex than in the free $tRNA^{Phe}$ (Figure 7a). Similarly, a higher thermal stability of the complex is reflected in the D-16(C_6) chemical shift temperature dependence. Whereas in the case of the free $tRNA^{Phe}$ a sharp transition occurs at 73 °C, melting in the complex is observed only at 78 °C (Figure 7b). No difference was observed between the melting of free $tRNA^{Phe}$ and the melting of $tRNA^{Phe}$·$tRNA^{Glu}$ when the temperature dependence of the m_2^2G-26 resonance was monitored. However, in this case the melting in free $tRNA^{Phe}$ already occurs at a higher temperature compared to the T-54 or D-16 resonances (Figure 7c).

(3) $tRNA^{Glu}$·$tRNA^{Phe}$ Anticodon Fragment Complex. Since the high-field spectral region of the $tRNA^{Glu}$·$tRNA^{Phe}$ complex was complicated by the strong broadening and overlapping of resonances at low temperature, we attempted to study the binding of the tRNA anticodon fragment (A-Cm-U-Gm-A-A-Y-A-Ψ-m^5C-U-Gp) to *E. coli* $tRNA^{Glu}$. Furthermore, the temperature-jump results of Grosjean et al. (1976) on the $tRNA^{Phe}$·$tRNA^{Glu}$ complex show that the constraint of the anticodon sequence into a hairpin loop accounts for a factor of 50 increase in the stability of the anticodon–anticodon complex. Hence, it would be of interest to observe the importance of loop closure on the stabilization of the tRNA·tRNA complex by NMR.

The temperature dependences of the high-field NMR spectra of the $tRNA^{Glu}$·$tRNA^{Phe}$ anticodon fragment are presented in Figure 10A. At 22 °C, the T-54 resonance in the complex is broadened but its resonance position remains unchanged. The m^5C peak in the complex experiences an upfield shift of 0.09 ppm compared to that seen in the free anticodon fragment. This observation indicates that the m^5C base is in an almost fully stacked conformation in the complex and that the strong stacking of the short anticodon–anticodon double helix is transmitted to the base m^5C which is four positions away. The C_{11}-CH_3, N_3-CH_3, and $COOCH_3$ resonances of the Y base move by 0.1, 0.08, and 0.02 ppm upfield, respectively, upon complex formation. The resonance due to the mam^{5}s^{2}U-34(NCH_3) clearly shifts downfield by 0.13 ppm. Figure 10B shows the melting of the $tRNA^{Glu}$·$tRNA^{Phe}$ anticodon fragment complex as a function of temperature as monitored by changes in the chemical shift of resonances from mam^{5}s^{2}U-34(NCH_3) and Y-37(C_{11}-CH_3). The NMR melting temperature of about 60 °C for the complex was estimated from the plots in Figure 10B. This is about 18 °C lower than the $tRNA^{Glu}$·$tRNA^{Phe}$ complex (Figure 9).

In the spectrum of the complex at 22 °C (Figure 10A), a broad resonance at 1.5 ppm appears which moves under the peak at 1.69 ppm at 42 °C. At 58 °C it superimposes the peak at 1.95 ppm and at 66 °C appears as a broad peak at 2.21 ppm. Finally, at 73 °C, this resonance moves to 2.3 ppm which is the resonance position for the nucleoside m^2A-37. If one tentatively assigned the peak at 1.5 ppm to the nucleoside m^2A in the $tRNA^{Glu}$·$tRNA^{Phe}$ anticodon fragment complex, it would imply an upfield shift of 0.8 ppm upon complexation. Since the nucleoside m^2A is positioned on the 3′ side of the anticodon at the end of the double helix, a large upfield shift upon complexation might be expected due to strong base stacking

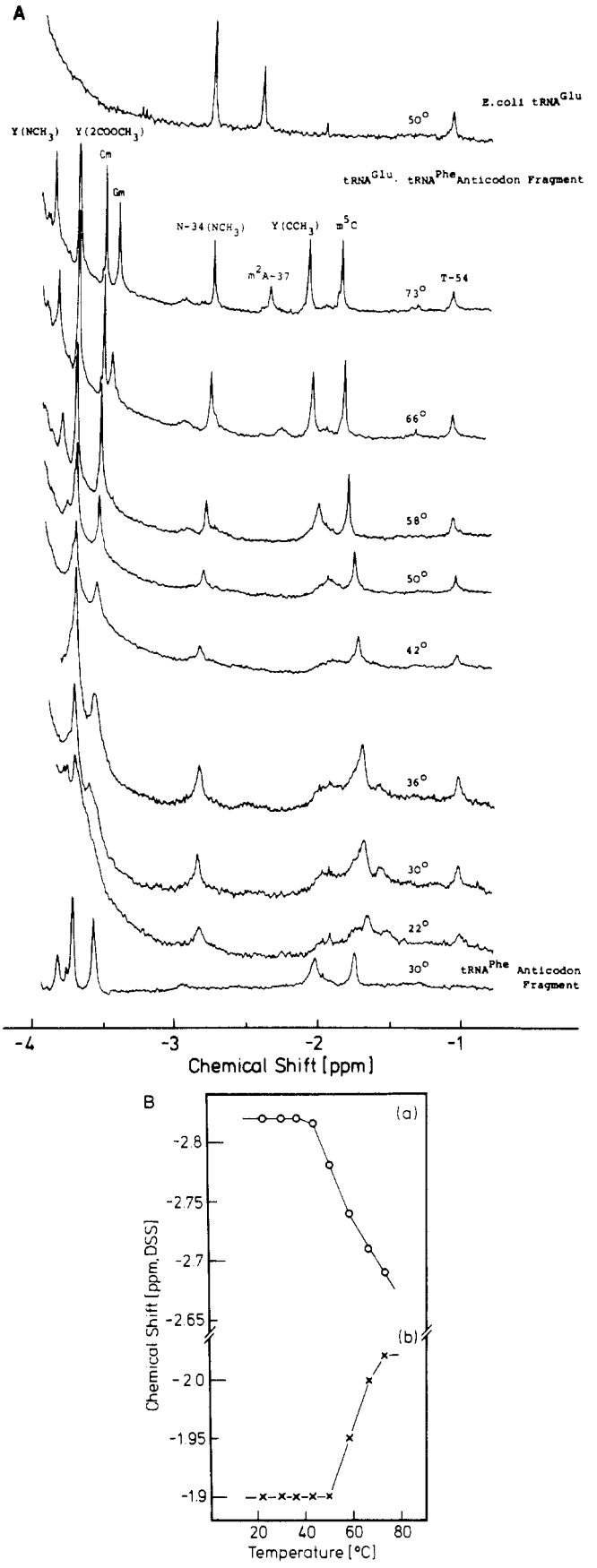

FIGURE 10: (A) Temperature dependence of high-field 270-MHz proton NMR spectrum of the *E. coli* $tRNA^{Glu}$·yeast $tRNA^{Phe}$ anticodon fragment complex, each 0.5 mM; (B) plot of the chemical shift as a function of temperature for the resonances (a) mam^{5}s^{2}U-34(NCH_3) proton and (b) Y(C_{11}-CH_3) proton in Figure 10A.

of this nucleoside on the short codon–anticodon double helix (Martin et al., 1971; Grosjean et al., 1976).

Discussion

The improvement in the resolution of the high-field NMR spectra and the complete assignment of the methyl and methylene resonances of native yeast tRNA^{Phe} provide a possibility of studying the structure of this tRNA in solution. In particular, information on the non-base-paired loop regions, which cannot be investigated by low-field NMR spectroscopy, can be obtained by monitoring the resonances of the methyl and methylene protons of the minor nucleosides.

In the present study we observed differences between the chemical shifts of the C_6 protons of the D-16 and D-17 residues of tRNA^{Phe}, an observation which was not made in similar previous NMR investigations (Kan et al., 1977; Robillard et al., 1977). In the X-ray crystal structure of tRNA^{Phe} from yeast (Holbrook et al., 1978), both D-16 and D-17 residues are free, without direct interaction with other parts of the molecule. Our NMR data suggest, however, that one of the D residues experiences a shielding effect from a neighboring base or through a tertiary interaction. By a comparative study using other tRNA species containing dihydrouridine residues, we suggest that it is the D-16 residue which is involved in some kind of higher structure. It is possible that the residue 16, being present in all tRNA species, participates in such an interaction whereas the residue 17, being part of one of the variable regions, is generally not involved in tertiary interactions. The shielding of the residue D-20 in tRNA^{fMet} from *T. thermophilus* and of the residue D-20 as well as D-20:1 in tRNA^{Ser} from yeast ($\Delta\delta \sim 0.5$ ppm) also suggests an involvement of these residues in the ordered structure.

At the present time we have not succeeded in interpreting the high-field NMR data in order to determine the structure of the anticodon loop in solution. This is due mostly to the limitation that NMR signals of the minor nucleosides present in the anticodon loop of tRNA^{Phe} overlap in the region of 3–4 ppm. The resolution in this region, especially at low temperature, is insufficient to permit an interpretation of the anticodon loop structure. Indirect evidence on the stacking pattern of the anticodon loop of tRNA^{Phe} in solution was obtained, however, by NMR measurement of tRNA^{Phe}(–Y). The stacking of the anticodon to the 3′ part of the anticodon loop, as apparent from the X-ray structure of tRNA^{Phe} (Quigley et al., 1978) probably also takes place in the intact tRNA^{Phe} in solution. This can be deduced from the large changes observed in the Gm-34 resonance of tRNA^{Phe}(–Y) as compared to native tRNA^{Phe}. These may be interpreted as caused by a disruption of the stacking of the anticodon to its 3′ neighbors in the anticodon loop. No changes were observed in the resonance of Cm-32 after removal of the Y base, implying that this residue is not influenced by the disturbance in the anticodon.

Komorowski & Allerhand (1972) determined the correlation time for the overall rotational reorientation of the folded tRNA molecule on the basis of ^{13}C relaxation values as being about 30 ns. Our calculated τ_c values of the minor nucleosides are shorter than that of the folded tRNA structure. This suggests that the minor nucleosides have a considerable degree of rotational freedom and are not immobilized in the tRNA structure. There are, however, differences in the correlation times for the minor nucleosides located in the different regions of tRNA. Whereas the side chain of the Y-37 base in the anticodon loop is less immobilized, the τ_c values of the bases involved in the tertiary structure core, T-54, m_2^2G-26, and m^2G-10, show a stronger immobilization. An intermediate τ_c for the two overlapping peaks of m^5C-40 and m^5C-49 probably reflects an average τ_c value of the more immobilized m^5C-49 and the less immobilized m^5C-40. These findings are in good agreement with the interpretation of the X-ray data of yeast tRNA^{Phe} by Holbrook et al. (1978), which suggest a higher radius of vibration of the residues at the two ends of the L-shaped molecule as compared to the nucleosides in the center of the tertiary structure. Exceptions from this rule are the minor nucleosides D-16 and D-17. The C_5 methylene groups of these residues exhibit a short τ_c of 5.7 ns. This indicates a high degree of rotational freedom of at least one of the dihydrouridine residues.

Several resonances in the region between 1.0 and 1.8 ppm were ascribed to the methyl group of the T-54 residue (Kastrup & Schmidt, 1978; Kan et al., 1977; Robillard et al., 1977). In the present study we performed a more careful investigation of this phenomenon which indicates multiple conformations of T-54 in tRNA. Under conditions where the tRNA^{Phe} is in its native form, i.e., at low temperature and in the presence of more than 50 mol of Mg^{2+} per mol of tRNA, only a single resonance for T-54 was observed at 1.0 ppm. Under these conditions the tRNA melts in a cooperative manner at about 75 °C. This transition is reflected by a broadening of NMR signals and the appearance of a T-54 resonance at 1.56 ppm. When the temperature is raised to 95 °C this resonance moves further, to 1.72 ppm, which is characteristic of unstructured tRNA^{Phe}. No further T-54 resonances could be detected below the T_m in the range 1.0–1.8 ppm, indicating that in a native tRNA^{Phe} only a single conformation of T-54 is present. By lowering the concentration of the Mg^{2+} to about 1 mol of Mg^{2+} or less per mol of tRNA, we found that the NMR melting of tRNA^{Phe} exhibits several transitions, and at a temperature around the first transition an intermediate conformation of T-54 can be observed which is reflected by a resonance at 1.3 ppm. Kastrup & Schmidt (1978) have recently investigated the thermal denaturation of tRNA$_1^{Val}$ from *E. coli* by high-field proton NMR. Under conditions where 0.4 mol of Mg^{2+} per mol of tRNA^{Val} was present, they observed several intermediate T-54 signals in a temperature range between 20 and 85 °C. It is therefore likely that the appearance of multiple T-54 resonances during the thermal denaturation of tRNA in the absence of Mg^{2+} or at very low Mg^{2+} concentrations is related to the structure of tRNA during its sequential melting (Crothers et al., 1974; Riesner et al., 1973).

In order to obtain information about the possible conformations of T-54 which give rise to the 1.0 and 1.3 ppm resonances in the yeast tRNA^{Phe} spectrum, we measured the fragment (47–76) of tRNA^{Phe}. This fragment is only able to form the hairpin structure of the T-Ψ-C arm and is obviously lacking the tertiary interactions (Römer et al., 1969). At low temperature (20–45 °C), this fragment gives rise to a T-54 resonance at 1.0 ppm together with other T-54 resonances at 1.28 and 1.32 ppm. This implies that the stabilization of the T-54 conformation as reflected by the 1.0-ppm resonance is adequately accomplished by the secondary structure. Consequently, we conclude that the major source of shielding of T-54 arises from the structural features of the T-Ψ-C loop and stem and not from the tertiary structural interaction. The different stacking modes of the T-54 over the G-53·C-61 base pair which is stabilized by a three-dimensional interaction are likely candidates for the source of the multiple resonances of T-54 (Figure 4).

In the three-dimensional structure of yeast tRNA^{Phe} (Holbrook et al., 1978), the T-54 is stacked between the G-53·C-61 and the Ψ-55·G-18 base pairs and is itself base-

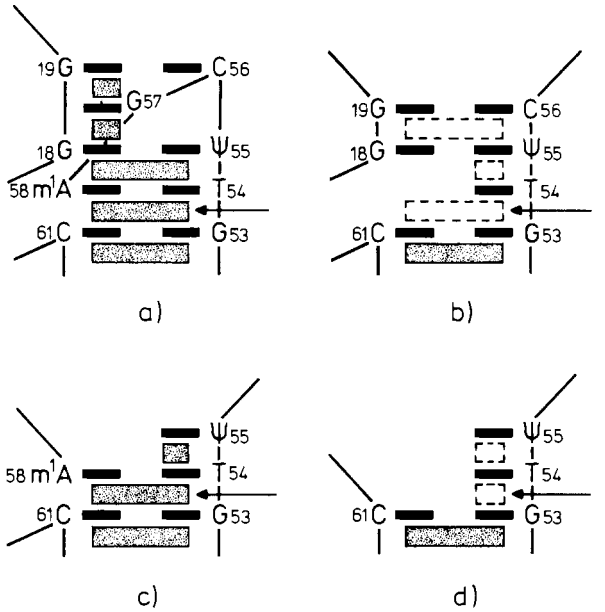

FIGURE 11: The probable hydrophobic stacking interaction of the T-54 residue (marked by arrow) in (a) intact yeast $tRNA^{Phe}$ according to Rich & RajBhandary (1976); (b) yeast $tRNA^{Phe}$ in which the m^1A-58·T-54 hydrogen bond is disrupted; (c) the (47–76) fragment of $tRNA^{Phe}$ and yeast $tRNA^{Phe}$ in which the base-pair interactions between the D loop and the T-Ψ-C loop are disrupted; and (d) the case of (c) but with the additional disruption of the m^1A-58·T-54 base pair.

paired with m^1A-58 (Figure 11a). On the basis of the ring current values (Giessner-Prettre et al., 1976), the 0.7-ppm upfield shift observed for the T-54 both in the intact $tRNA^{Phe}$ and in the fragment (47–76) of $tRNA^{Phe}$ must originate from stacking on the G-53·C-61 base pair. In the intact tRNA the relative orientation of the T-54 base is stabilized by tertiary interactions between the dihydrouridine and the T-Ψ-C loops, resulting in a particular conformation of the T-54 (Figure 11a). In the free T-Ψ-C loop, after melting of the tertiary structure, and in the fragment (47–76) of $tRNA^{Phe}$, the T-54 probably changes its stacking interaction with the base pair G-53·C-61 (Figure 11c,d), thus explaining the multiple resonances for T-54.

Our observation that in the aminoacylated Phe-$tRNA^{Phe}$-C-C-A(3′NH_2), in the presence of an excess of Mg^{2+}, T-54 can adopt a less-stable conformation as reflected by the appearance of the 1.3-ppm resonance might suggest that the aminoacylation produces a rearrangement in the tertiary structure of $tRNA^{Phe}$. This structural change influences the stacking interaction of T-54 with the G-53·C-61 base pair (Figure 11b). Since Phe-$tRNA^{Phe}$-C-C-A(3′NH_2) is not able to bind oligonucleotides which are complementary to the T-Ψ-C loop (Pongs et al., 1976), a disruption of the tertiary structure of this tRNA is not likely. On the other hand, the recent work of Potts et al. (1977) indicates that there is a change in the shape of the tRNA molecule upon aminoacylation which can only be detected at defined Mg^{2+} concentrations.

With regard to the correlation between the magnesium ions binding and the aminoacylation of tRNA, Ninio et al. (1972), using small-angle X-ray scattering, have reported that aminoacylation causes the tRNA molecule to undergo small structural changes which affect the distribution of the charged groups on the outer surface of the molecule and hence the Mg^{2+} binding. Furthermore, Cohn et al. (1969) have reported that the number of manganese binding sites changed on aminoacylation. It is possible that changes in the Mg^{2+} binding sites in the vicinity of the T-Ψ-C loop (Ninio et al., 1972) may influence the conformation of the T-54 residue. The present evidence for the structure of aminoacyl-tRNA [Potts et al. (1977) and references cited therein] suggests that a subtle conformational change of the tRNA takes place upon aminoacylation without a large rearrangement of the tertiary structure. Our investigation indicates that such a conformational change affects the T-54 residue.

The fact that a structural modification of the tRNA can influence the resonances of the residues far distant from the point of modification was demonstrated by the high-field NMR spectrum of $tRNA^{Phe}$(−Y) and of the $tRNA^{Phe}$·$tRNA^{Glu}$ complex. The temperature-induced melting of the $tRNA^{Phe}$(−Y), as monitored by the changes in the chemical shift of D-16(C_6), T-54, and m_2^2G-26 resonances, occurs at a lower temperature as compared to native $tRNA^{Phe}$. This indicates that a structural disturbance in the anticodon loop may result in long-range effects in the remote parts of the molecule. Whereas by excision of the Y base the thermal stability in the T-Ψ-C, D-16, and m_2^2G-26 regions is decreased, an opposite effect was observed in the case of the $tRNA^{Phe}$·$tRNA^{Glu}$ complex. Here the thermal unfolding, as monitored by T-54 and D-16(C_6) resonances, takes place at a higher temperature as compared to free $tRNA^{Phe}$.

Thus, an involvement of the anticodon of $tRNA^{Phe}$ in a base-pairing interaction induces a significant stabilization of the $tRNA^{Phe}$ structure against thermal unfolding, and, furthermore, no conformational changes in T-54 could be detected upon the $tRNA^{Phe}$·$tRNA^{Glu}$ complex formation. Our study therefore contradicts the hypothesis that the codon–anticodon interaction may trigger an unfolding of the tertiary structure of tRNA and induce accessibility of the T-Ψ-C region (Schwarz et al., 1976; Schwarz & Gassen, 1977; Wagner & Garrett, 1978). This may, however, be due to the limitations of our model system involving tRNA species with complementary anticodons. On the other hand, it is also likely that other components involved in the ribosomal decoding process as well as the proper codon are necessary to induce the conformational change needed for the proper binding of the aminoacyl-tRNA to the ribosomal A site (Sprinzl et al., 1976).

Very recently, a report appeared (Geerdes et al., 1978) concerning an NMR study of the interaction of the anticodon of yeast $tRNA^{Phe}$ with the oligonucleotide UpUpCpA. The low-field proton spectra of the yeast $tRNA^{Phe}$ indicated, in good agreement with our results, no loss of hydrogen-bonded proton resonances. This implies that the hydrogen bonds between the D and the T-Ψ-C loops which are necessary for stabilization of the tertiary structure of $tRNA^{Phe}$ remain intact after the binding of this oligonucleotide to the anticodon.

A preliminary NMR study in the high- and low-field spectra of Phe-$tRNA^{Phe}$-C-C-A(3′NH_2) has been performed by Kan et al. (1976). These authors observed that two resonances in the low-field spectrum were changed upon aminoacylation of $tRNA^{Phe}$-C-C-A(3′NH_2) but no differences in the high-field spectrum could be identified. This may be due to the lower resolution of the high-field NMR spectrum at low temperatures (as compared to the present study) or to impurities in the sample of aminoacylated $tRNA^{Phe}$ masking that part of the NMR spectrum where the T-54 resonance occurs.

The observed differences in the low-field part of the spectrum described by Kan et al. (1976) indicated a conformational change of tRNA-C-C-A(3′NH_2) upon aminoacylation, which is in good agreement with our present study.

Acknowledgments

We are grateful to Dr. F. von der Haar for providing us with highly purified yeast tRNA^{Phe}. We thank Drs. D. Gauss and G. Igloi for the critical reading of the manuscript and E. Graeser and M. Kucharzewski for the preparation of tRNAs. We thank Dr. R. Perraud for his collaboration in the initial stage of this work.

References

Abragam, A. (1967) *The Principles of Nuclear Magnetism*, p 64, Oxford University Press, Oxford.

Allerhand, A., Doddrell, D., Glushko, V., Cochran, D. W., Wenkert, E., Lawson, P. J., & Gurd, F. R. N. (1971) *J. Am. Chem. Soc., 93*, 544–546.

Burke, T. E., & Chan, S. I. (1970) *J. Magn. Reson. 2*, 120–140.

Chin, R. C., & Kidson, C. (1971) *Proc. Natl. Acad. Sci. U.S.A. 68*, 2448–2452.

Cohn, M., Danchin, A., & Grunberg-Manago, M. (1969) *J. Mol. Biol. 39*, 199–217.

Crothers, D. M., Cole, P. E., Hilbers, C. W., & Shulman, R. G. (1974) *J. Mol. Biol. 87*, 63–88.

Davanloo, P., Sprinzl, M., Watanabe, K., Albani, M., & Kersten, H. (1979) *Nucleic Acids Res. 6*, 1571–1581.

Dvorak, D. J., Kidson, C., & Chin, R. C. (1976) *J. Biol. Chem. 251*, 6730–6734.

Eisinger, J. (1971) *Biochem. Biophys. Res. Commun. 43*, 854–861.

Eisinger, J., & Gross, N. (1975) *Biochemistry 14*, 4031–4041.

Gauss, D. H., Grüter, F., & Sprinzl, M. (1979) *Nucleic Acids Res. 6*, r_1–r_{19}.

Geerdes, H. A. M., Van Boom, J. H., & Hilbers, C. W. (1978) *FEBS Lett. 88*, 27–32.

Giessner-Prettre, C., Pullman, B., Borer, P. N., Kan, L. S., & Ts'o, P. O. P. (1976) *Biopolymers 15*, 2277–2286.

Grosjean, H., Söll, D. G., & Crothers, D. M. (1976) *J. Mol. Biol. 103*, 499–519.

Gutowsky, H. S., & Woessner, D. E. (1956) *Phys. Rev. 104*, 843–844.

Holbrook, S. R., Sussman, J. L., Warrant, R. W., & Kim, S. H. (1978) *J. Mol. Biol. 123*, 631–660.

Jack, A., Ladner, J. E., & Klug, A. (1976) *J. Mol. Biol. 108*, 619–649.

Kan, L. S., Ts'o, P. O. P., Sprinzl, M., von der Haar, F., & Cramer, F. (1976) *Biophys. J. 16*, 11a.

Kan, L. S., Ts'o, P. O. P., Sprinzl, M., von der Haar, F., & Cramer, F. (1977) *Biochemistry 16*, 3143–3153.

Kastrup, R. V., & Schmidt, P. G. (1978) *Nucleic Acids Res. 5*, 257–269.

Komoroski, R. A., & Allerhand, A. (1972) *Proc. Natl. Acad. Sci. U.S.A. 69*, 1804–1808.

Kruse, T. A., Clark, B. F. C., & Sprinzl, M. (1978) *Nucleic Acids Res. 5*, 879–892.

Maelicke, A., von der Haar, F., & Cramer, F. (1973) *Biopolymers 12*, 27–43.

Martin, F. H., Uhlenbeck, O. C., & Doty, P. (1971) *J. Mol. Biol. 57*, 201–215.

Möller, A., Schwarz, U., Lipecky, R., & Gassen, H. G. (1978) *FEBS Lett. 89*, 263–266.

Ninio, J., Luzzati, V., & Yaniv, M. (1972) *J. Mol. Biol. 71*, 217–229.

Nishimura, S. (1971) in *Procedures in Nucleic Acids Research* (Cantoni, G. L., & Davies, D. R., Eds.) pp 542–564, Harper and Row, New York.

Pongs, O., Bald, R., & Reinwald, E. (1973) *Eur. J. Biochem. 32*, 117–125.

Pongs, O., Wrede, P., Erdmann, V. A., & Sprinzl, M. (1976) *Biochem. Biophys. Res. Commun. 71*, 1025–1033.

Potts, R., Fournier, M. J., & Ford, N. C. (1977) *Nature (London) 268*, 563–564.

Quigley, G. J., Wang, A. H. J., Seeman, N. C., Suddath, F. C., Rich, A., Sussman, J. L., & Kim, S. H. (1975) *Proc. Natl. Acad. Sci. U.S.A. 72*, 4866–4870.

Quigley, G. J., Teeter, M. M., & Rich, A. (1978) *Proc. Natl. Acad. Sci. U.S.A. 75*, 64–68.

RajBhandary, U. L., Stuart, A., & Chang, S. H. (1968) *J. Biol. Chem. 243*, 584–591.

Rich, A., & RajBhandary, U. L. (1976) *Annu. Rev. Biochem. 45*, 805–860.

Richter, D., Erdmann, V. A., & Sprinzl, M. (1973) *Nature (London), New Biol. 246*, 132–135.

Richter, D., Erdmann, V. A., & Sprinzl, M. (1974) *Proc. Natl. Acad. Sci. U.S.A. 71*, 3226–3229.

Riesner, D., Maass, G., Thiebe, R., Phillippsen, P., & Zachau, H. G. (1973) *Eur. J. Biochem. 36*, 76–88.

Robertson, J. M., Kahan, M., Wintermeyer, W., & Zachau, H. G. (1977) *Eur. J. Biochem. 72*, 117–125.

Robillard, G. T., Tarr, C. E., Vosman, F., & Reid, B. R. (1977) *Biochemistry 16*, 5261–5273.

Roe, B., Marcu, K., & Dudock, B. (1973) *Biochim. Biophys. Acta 319*, 25–36.

Römer, R., Riesner, D., Maass, G., Wintermeyer, W., Thiebe, R., & Zachau, H. G. (1969) *FEBS Lett. 5*, 15–19.

Schneider, D., Solfert, R., & von der Haar, F. (1972) *Hoppe-Seyler's Z. Physiol. Chem. 353*, 1330–1336.

Schwarz, U., & Gassen, H. G. (1977) *FEBS Lett. 78*, 267–270.

Schwarz, U., Lührmann, R., & Gassen, H. G. (1974) *Biochem. Biophys. Res. Commun. 56*, 807–814.

Schwarz, U., Menzel, H. M., & Gassen, H. G. (1976) *Biochemistry 15*, 2484–2490.

Sprinzl, M., & Cramer F. (1973) *Nature (London), New Biol. 245*, 3–5.

Sprinzl, M., Wolfrum, D. I., & Neuhoff, V. (1975) *FEBS Lett. 50*, 54–56.

Sprinzl, M., Wagner, T., Lorenz, S., & Erdmann, V. A. (1976) *Biochemistry 15*, 3031–3039.

Sprinzl, M., Sternbach, H., von der Haar, F., & Cramer, F. (1977) *Eur. J. Biochem. 81*, 579–589.

Thiebe, R., & Zachau, H. G. (1968) *Eur. J. Biochem. 5*, 546–555.

Uziel, M., Koh, C. K., & Cohn, W. E. (1968) *Anal. Biochem. 25*, 77–98.

van Geet, A. L. (1968) *Anal. Chem. 40*, 2227–2229.

Vold, R. L., Waugh, J. S., Klein, M. P., & Phelps, D. E. (1968) *J. Chem. Phys. 48*, 3831–3832.

Wagner, R., & Garrett, R. A. (1978) *FEBS Lett. 85*, 291–295.

Watanabe, K., Kuchino, Y., Yamaizumi, Z., Kato, M., Oshima, T., & Nishimura, S. (1978) *Nucleic Acids Res. 5*, s473–s476.

Wintermeyer, W., & Zachau, H. G. (1970) *FEBS Lett. 11*, 160–164.

Woessner, D. E. (1962) *J. Chem. Phys. 37*, 1–4.